Characterization of a correlated topological Kondo insulator in one dimension

I. Hagymási and Ö. Legeza

Strongly Correlated Systems "Lendület" Research Group, Institute for Solid State Physics and Optics,
MTA Wigner Research Centre for Physics, Budapest H-1525 P.O. Box 49, Hungary

We investigate the ground state of a p-wave Kondo-Heisenberg model introduced by Alexandrov and Coleman with an Ising-type anisotropy in the Kondo interaction and correlated conduction electrons. Our aim is to understand how they affect the stability of the Haldane state obtained in the SU(2)-symmetric case without the Hubbard interaction. By applying the density-matrix renormalization group algorithm and calculating the entanglement entropy we show that in the anisotropic case a phase transition occurs and a Néel state emerges above a critical value of the Coulomb interaction. These findings are also corroborated by the examination of the entanglement spectrum and the spin profile of the system which clarify the structure of each phase.

I. INTRODUCTION

Kondo insulators are semiconductors at low temperatures with a few meV gap in contrast to the conventional semiconductors in which the gap is on the order of a few eV [1]. It is now generally accepted that strong correlations among the electrons lead to the stabilization of this state with such a small gap [2].

In the last decade a new group of insulators have been discovered, which are gapped in the bulk, but they have soft, topologically protected surface states [3–5]. They are the topological insulators whose basic properties can be understood within the framework of ordinary band theory. The question naturally arises as to how the correlation among the electrons affects the properties of topological insulators. This aspect has attracted significant attention [6–13] since the existence of topological phases was suggested in strongly correlated systems [14–18]. These observations made it necessary to understand, *inter alia*, the theoretical properties of topological Mott [6,19–22] and Kondo insulators [23–29]. The most famous example of topological Kondo insulators is SmB_6, which was discovered more than four decades ago [30]. Recent experimental observations [31–33] that SmB_6 can host robust conducting surface states renewed the interest in this compound in particular and in Kondo insulators in general [34–36]. The most important aspect of topological Kondo insulators is that hybridization occurs between d and f bands whose parities are opposite to each other [29]. This leads to the appearance of a symmetry-protected topological ground state [28].

To capture the effects of strong correlations and topology simultaneously, Alexandrov and Coleman suggested a Kondo lattice model with a special form of the Kondo exchange [24]. The model consists of a free one-dimensional electron gas coupled to an $S = 1/2$ Heisenberg chain via a Kondo exchange with p-wave character. In the conventional Kondo lattice model, where the Kondo exchange is on-site, local singlets are formed in the strong-coupling limit and the boundaries do not play an important role. In contrast, in the present case since they become nonlocal, these singlets are broken at the boundary, and edge states appear [24]. This p-wave Kondo-Heisenberg model has been investigated with several methods. The large-N expansion has revealed that magnetic

end states appear at the boundaries [24]. Analyzing the ground state with Abelian bosonization [28] and the density-matrix renormalization group (DMRG) algorithm [37], it has turned out that the ground state is actually the Haldane phase [38,39]. It is also interesting to mention that the Haldane phase has been previously observed in the ordinary Kondo lattice model with ferromagnetic Kondo coupling [40] and in the extended periodic Anderson model with Hund's coupling [41]. The facts above clearly indicate that one has to apply sophisticated many-body techniques to accurately describe the ground state.

In this paper our aim is to study the stability of the Haldane phase against perturbations. The most obvious and physically relevant choices are either to introduce anisotropy in the Kondo interaction or the inclusion of a Coulomb interaction in the conduction band. The role of the Coulomb interaction was explored in the case of the conventional Kondo lattice model [42,43], but only the weak-coupling limit of the present model has been studied so far with bosonization [28]. In contrast, the anisotropy was studied only in the conventional model and its phase diagram was determined [44–46]. We address these problems using the DMRG algorithm [47–51], which is the state-of-the-art tool to determine the ground state and it makes it possible to go beyond the weakly interacting limit. Since the DMRG calculation is closely related to quantum information theory, we can determine the entanglement entropy [52–57] and entanglement spectrum [58], which are very useful to detect quantum phase transitions [59–62] and symmetry-protected topological order [63–65]. Our analysis of the anisotropic model reveals that (i) a phase transition occurs as the interaction is increased within the conduction band and the Haldane state transforms into a Néel state, and (ii) the entanglement spectrum can be used as a fingerprint to identify a topological Kondo insulator in one dimension.

The setup of the paper is as follows. In Sec. II the model is introduced and some details of the DMRG calculation and quantum information theory are given. In Sec. III A our results are presented for the isotropic model and we determine the low-lying excitation spectrum. In Sec. III B the role of the anisotropy is addressed using the elements of quantum information theory to identify topological order and quantum phase transitions. Finally, in Sec. IV we give the conclusions of this work.

II. MODEL

The Hamiltonian of the p-wave Kondo-Heisenberg model in one dimension can be written as

$$H = H_c + H_H + H_K, \tag{1}$$

where

$$H_c = -t \sum_j (c_{j+1\sigma}^\dagger c_{j\sigma} + c_{j\sigma}^\dagger c_{j+1\sigma}) + U \sum_j n_{j\uparrow} n_{j\downarrow} \tag{2}$$

describes the interacting conduction band, with nearest-neighbor hopping t and Hubbard repulsion U. The Hamiltonian

$$H_H = J_H \sum_j \mathbf{S}_j \cdot \mathbf{S}_{j+1} \tag{3}$$

contains the Heisenberg interactions between the $S = 1/2$ spins, with $J_H > 0$. Finally, H_K couples the two subsystems via an anisotropic, nonlocal Kondo exchange introduced between electronic and spin degrees of freedom, in a manner similar to that in Ref. [44]:

$$H_K = J_K \sum_j \left[\frac{1}{2}(S_j^+ \pi_j^- + S_j^- \pi_j^+) + \Delta S_j^z \pi_j^z \right], \tag{4}$$

where Δ is the strength of the Ising-type anisotropy, and $S_j^\pm$ and $\pi_j^\pm$ (S_j^z and π_j^z) are the ladder operators (z components) of the spin $\mathbf{S}_j$ and the p-wave spin density $\boldsymbol{\pi}_j$:

$$\boldsymbol{\pi}_j = \frac{1}{2} \sum_{\alpha\beta} p_{j\alpha}^\dagger \boldsymbol{\sigma}_{\alpha\beta} p_{j\beta}. \tag{5}$$

Here $\boldsymbol{\sigma}$ is the vector of Pauli matrices and

$$p_{j\sigma} \equiv (c_{j+1\sigma} - c_{j-1\sigma})/\sqrt{2}, \tag{6}$$

where $c_{0\sigma} = c_{L+1\sigma} = 0$ is assumed. The present Kondo exchange, in contrast to the usual s-wave case, couples the localized spins to the corresponding p-wave spin densities in the fermionic subsystem. As a result, the Kondo interaction now contains an exchange term between $\mathbf{S}_j$ and the conduction electron spins $\mathbf{s}_{j-1}$, $\mathbf{s}_{j+1}$, where

$$\mathbf{s}_j = \frac{1}{2} \sum_{\alpha\beta} c_{j\alpha}^\dagger \boldsymbol{\sigma}_{\alpha\beta} c_{j\beta}. \tag{7}$$

In addition, a new kind of process appears, where an electron can hop to its next-nearest neighbor while the intermediate spin is flipped.

The conventional one-dimensional Kondo lattice model was thoroughly investigated in the half-filled and in the metallic case [40,66] and no topological order was found. The role of the correlation between the conduction electrons was also addressed and its effect can be considered as the renormalization of the spin and charge gaps [66]. There are, however, only a few studies available on the p-wave Kondo-Heisenberg model [24,28,37] and the role of the interaction between the conduction electrons has been studied only in the weakly interacting case. Furthermore, the effect of the anisotropy in the present model is a completely open question.

We applied the DMRG algorithm using the dynamic block-state selection approach [67,68] to study the ground state of the Hamiltonian in Eq. (1). In our calculation the *a priori* value of the quantum information loss, χ, was set to $\chi = 10^{-5}$, and the truncation errors were on the order of magnitude of 10^{-7}. We considered chains with open boundary conditions up to lengths $L = 600$. In what follows we use the half bandwidth $W = 2t$ as the energy scale and set $J_H = 0.5W$, $J_K = W$ and vary the anisotropy and the Hubbard interaction strength. We consider the half-filled case and $\Delta \geqslant 1$.

It has been shown recently [63–65] that studying the bipartite entanglement of the ground-state wave function is a powerful tool to identify topological phases. Namely, the degeneracy of the entanglement spectrum, which is obtained from the Schmidt values, can be used to characterize the topological order. Therefore changes in the character of the whole entanglement spectrum must be accompanied by a phase transition, where either a level-crossing occurs or the correlation length diverges. We study the entanglement between the two halves of the chain. To this end we determine the von Neumann entropy of the half chain (block entropy) [52,53,55]:

$$s(L/2) = -\mathrm{Tr}\, \rho_{L/2} \ln \rho_{L/2} = -\sum_j \Lambda_j \ln \Lambda_j, \tag{8}$$

where $\rho_{L/2}$ is the reduced density matrix belonging to the half chain and Λ_j are the corresponding eigenvalues which are the squares of the Schmidt values.

III. RESULTS

A. Isotropic case

First, we examined the SU(2)-symmetric case ($\Delta = 1$) and calculated the entanglement spectrum as a function of U as can be seen in Fig. 1. It is known that one hallmark of the Haldane phase is its exactly evenly degenerate entanglement spectrum [63], which is obvious from Fig. 1. Note that our result provides further independent evidence for the Haldane phase at $U = 0$, which was previously identified by its
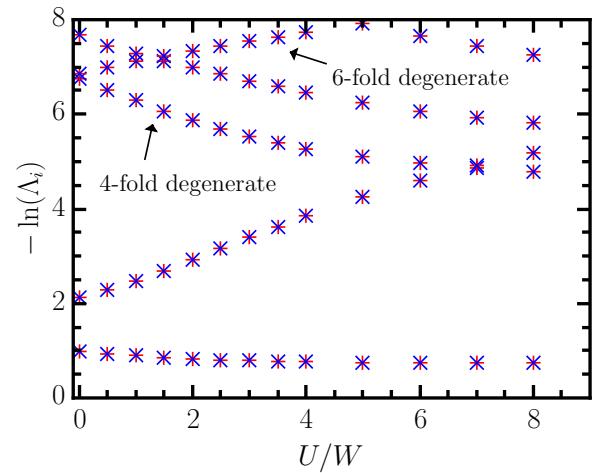

FIG. 1. The low-lying entanglement spectrum in the isotropic case extrapolated to the thermodynamic limit for $J_K = W$ and $J_H = 0.5W$. For better visibility of the degeneracies, the subsequent eigenvalues are denoted by $+$ and $\times$ symbols, respectively. In certain cases, where the multiplicity is larger than 2, the degree of degeneracy is given explicitly in the figure.
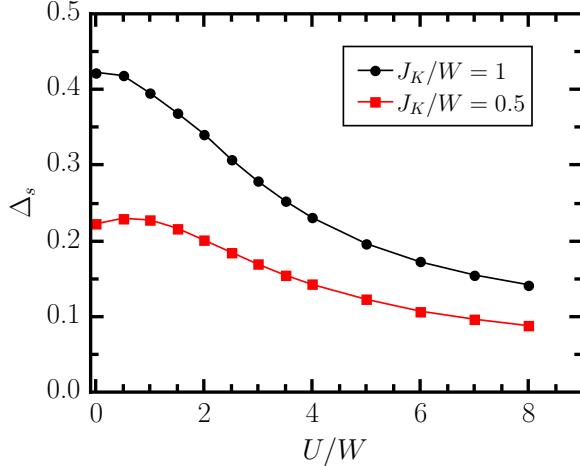
FIG. 2. The spin gap (extrapolated to the thermodynamic limit) in the isotropic model as a function of U for various J_K and $J_H = 0.5W$. The lines are guides to the eye.

nonvanishing string order parameter [37]. Besides that, it is clearly observed from Fig. 1 that the Haldane phase is realized not only for small U but for any $U \geqslant 0$, which is clearly beyond the validity of the bosonization approach [28]. One can naturally ask how the energy scales are modified after switching on U. The spin gap, Δ_s, which in our case can be identified with the Haldane gap (the singlet-quintet gap), decreases as is shown in Fig. 2. This can be understood from the large-U limit of the present model since it becomes equivalent to a diagonal spin ladder where the H_c Hamiltonian can be approximated with an $S = 1/2$ Heisenberg model with $J_c \sim 1/U$ [69]. It is interesting to remark that the Hubbard interaction leads to the increase of the spin gap in the conventional model [66].

B. Anisotropic case

As a next step we investigated what happens when the Kondo interaction becomes anisotropic ($\Delta \geqslant 1$). We calculated the block entropy for several chain lengths as a function of U, which is shown in Fig. 3. It is clearly observed that for short chains they do not exhibit anomalous behavior; however, a peak is developed as the chain length is increased. We know that extrema in the block entropy can be attributed to quantum critical points [55] if they evolve into anomalies in the thermodynamic limit. In the present case due to the anisotropy, a phase transition occurs at $U_c \approx 2.13W$, which separates two distinct phases. To detect symmetry-protected topological phases, we calculated again the entanglement spectrum, and its low-lying part is shown in Fig. 4 as a function of U. It is clear from Fig. 4 that the Haldane phase at $U = 0$ is not destroyed by the anisotropy; it survives even at $\Delta = 2$. Switching on U does not lead to drastic changes as long as $U < U_c$. Above this value a new phase emerges, where the topological order is no longer present, since both odd and even degeneracies occur in the entanglement spectrum.

To gain further insight into the properties of the two phases, we have calculated the low-lying excitation spectrum in each phase for $\Delta = 2$. More precisely, we considered the following
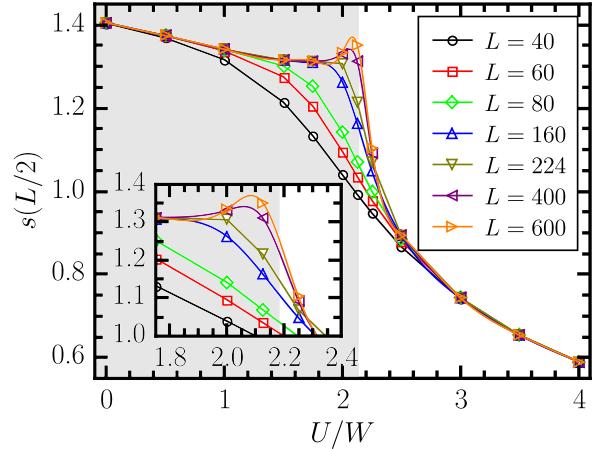

FIG. 3. The main figure shows the block entropy in the anisotropic case as a function of U for several chain lengths and $\Delta = 2$, $J_K = W$, $J_H = 0.5W$. The lines are the spline fit to the data points. The inset shows the enlarged region around the critical point.

energy gaps:

$$\Delta_{KL,MN} = E_L(T^z = K) - E_N(T^z = M). \quad (9)$$

Here T^z denotes the z component of the total spin:

$$\mathbf{T} = \sum_j \mathbf{T}_j \equiv \sum_j (\mathbf{S}_j + \mathbf{s}_j); \quad (10)$$

furthermore, $E_L(T^z = K)$ denotes the Lth energy level ($L = 1, 2, \ldots$) in the sector $T^z = K$. First, we consider the energy spectrum for $U = 0$, which is shown in Fig. 5. In the Haldane phase the ground state is expected to be fourfold degenerate if the open boundary condition is applied. For short chains a finite gap is observed, since the end spins are correlated; however, it closes exponentially, as the chain length is increased.
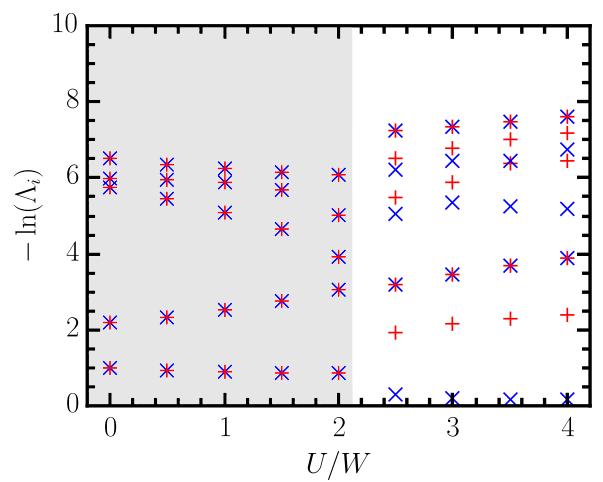

FIG. 4. The ten largest values of entanglement spectrum extrapolated to the thermodynamic limit as a function of U for $\Delta = 2$, $J_K = W$, $J_H = 0.5W$. For better visibility of the degeneracies, the subsequent eigenvalues are denoted by $+$ and $\times$ symbols, respectively.
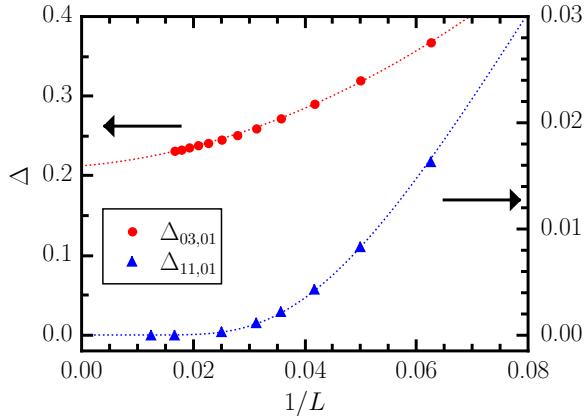
FIG. 5. Various gap values as a function of inverse chain length for $U = 0$ and $J_K = W$, $J_H = 0.5W$ for chains with up to $L = 80$ lattice sites. The dotted lines denote the best fits to the data using Eqs. (11) and (12) (see text).

FIG. 7. The total spin z component (T_i^z) along a finite chain with $L = 60$ sites and for different values of U. The symbols $\circ$, $\square$, and $\triangle$ denote $U/W = 0$, 1, and 3, respectively. The other parameters are $J_K = W$, $\Delta = 2$, $J_H = 0.5W$ in all cases.

Therefore these values can be fitted by

$$\Delta_{11,01}(L) = \Delta_{11,01} + A \exp(-\xi/L), \quad (11)$$

where fitting parameters are $\Delta_{11,01} = 8(6) \times 10^{-5}$, $A = 0.266(4)$, and $\xi = 0.174(1)$. Since the fitted value of $\Delta_{11,01}$ lies within the error margin of the energy values (determined by truncation error), we conclude that it is zero. Similar considerations apply for $\Delta_{02,01}$ (not shown). That is, the fourfold degeneracy is fulfilled in the thermodynamic limit. On the other hand, the gap between the ground state and the third excited state in the $T^z = 0$ sector is finite and its thermodynamic value can be obtained using the usual quadratic fit:

$$\Delta_{03,01}(L) = \Delta_{03,01} + B/L + C/L^2, \quad (12)$$

with best-fit parameters $\Delta_{03,01} = 0.212(1)$, $B = 0.60(8)$, and $C = 30(1)$. This gap can be identified as the Haldane gap in the anisotropic system.
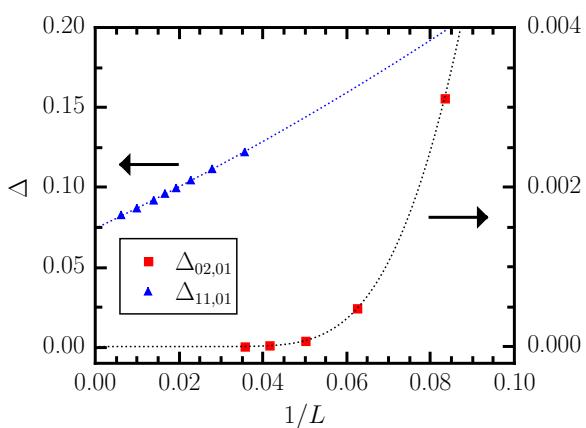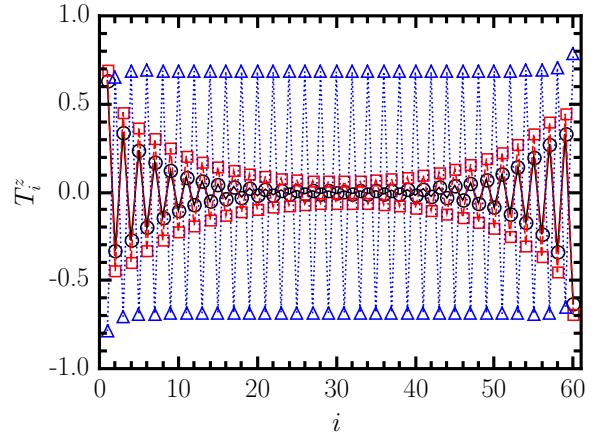
As a next step we consider what happens when $U > U_c$. From Fig. 6, it is seen that the ground state is twofold degenerate and the gap $\Delta_{11,01}$ remains finite. This was concluded from the size dependence of the gaps $\Delta_{02,01}$ and $\Delta_{11,01}$ which can be fitted using Eqs. (11) and (12), respectively. The best-fit parameters in this case are $A = 0.861(1)$, $\xi = 0.4685(1)$, and $\Delta_{02,01} = 4(1) \times 10^{-7}$ with Eq. (11), while $\Delta_{11,01} = 0.0743(3)$, $B = 1.24(3)$, and $C = 2.7(8)$ values are obtained with Eq. (12). The tiny gap in the former case is considered to be zero based on the previous arguments.

To explore the intrinsic properties of the new phase for $U > U_c$, we investigated the z component of the local magnetization, T_j^z, along the chain, which is shown in Fig. 7. One can easily see that for $U = 0$, finite spin polarization appears only at the edges. This is a well-known feature of the Haldane phase. Since our calculation was performed with zero total magnetization, the accumulated $1/2$ spins at the boundaries are aligned opposite to each other. As U is
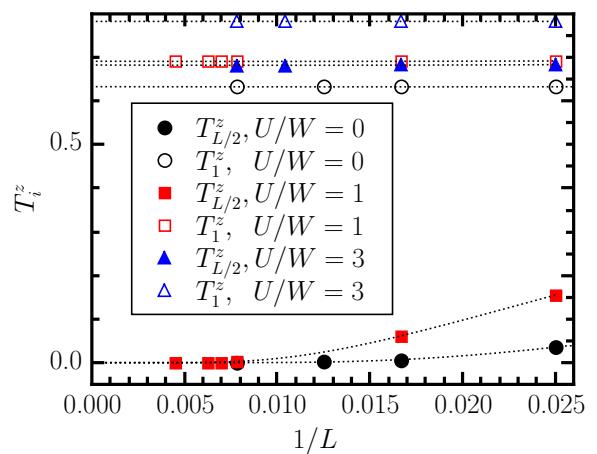

FIG. 6. Various gap values as a function of inverse chain length for $U = 3W$ and $J_K = W$, $J_H = 0.5W$ for chains with up to $L = 160$ lattice sites. The dotted lines denote the best fits to the data using Eqs. (11) and (12) (see text).

FIG. 8. Finite-size scaling of T_i^z values at the end of the chain (open symbols) and in the bulk (filled symbols) for different values of U up to $L = 224$ sites. The other parameters are $J_K = W$, $\Delta = 2$, $J_H = 0.5W$ in all cases.
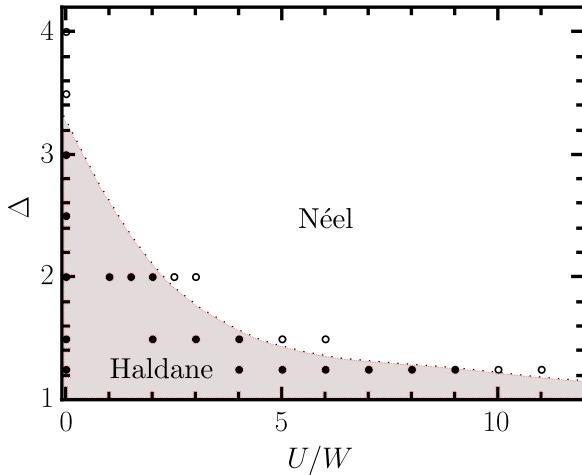
FIG. 9. The phase diagram of the anisotropic model as functions of the anisotropy and the Hubbard interaction strength for $J_K = W$ and $J_H = 0.5W$. The filled and open circles correspond to Haldane and Néel ground state, respectively. The dotted line denotes the approximate phase boundary.

increased the edge spins penetrate more and more into the bulk. To eliminate the finite-size effects we investigated how the local magnetization behaves in the thermodynamic limit both in the bulk and at the edges. It turns out from Fig. 8 that a finite spin polarization appears in the bulk for $U > U_c$. That is, the ground state for $U > U_c$ becomes a Néel state, which is expected to be twofold degenerate [70], as was confirmed by the analysis of the gaps. The topological Kondo insulator becomes a topologically trivial bulk insulator as the interaction is increased.

Finally, we investigated how the critical U depends on the anisotropy. The results are summarized in the phase diagram

in Fig. 9. It is interesting to note that for a weakly correlated conduction band the Haldane phase extends to much larger anisotropy values than for strong interaction. Note that the phase boundary between the Haldane and Néel state in the large-U limit remains at $\Delta > 1$, similarly as in the case of the $S = 1$ XXZ chain [71].

IV. CONCLUSIONS

We investigated the ground state and the first few excited states of a one-dimensional p-wave Kondo-Heisenberg model. We demonstrated that the anisotropic Kondo interaction and the correlation between conduction electrons affect the topological properties of the ground state. In the isotropic case we pointed out that the Hubbard interaction does not alter the topological properties of the ground state; however, it reduces the Haldane gap. In contrast, in the anisotropic case analyzing the block entropy, we showed that a phase transition occurs as U is increased. This was also corroborated by the analysis of the gaps and the change in the structure of the entanglement spectrum. The investigation of the local magnetization confirmed that the Néel phase appears in a certain parameter range. The effect of the anisotropy and the Hubbard interaction was summarized in a phase diagram. It is worth emphasizing that when the Hubbard interaction is weak the Haldane insulator state is realized in a much wider anisotropy range than in the strongly correlated case.

[1] P. S. Riseborough, Adv. Phys. **49**, 257 (2000).

[2] H. Tsunetsugu, M. Sigrist, and K. Ueda, Rev. Mod. Phys. **69**, 809 (1997).

[3] J. E. Moore, Nature (London) **464**, 194 (2010).

[4] M. Z. Hasan and C. L. Kane, Rev. Mod. Phys. **82**, 3045 (2010).

[5] X.-L. Qi and S.-C. Zhang, Rev. Mod. Phys. **83**, 1057 (2011).

[6] D. Pesin and L. Balents, Nat. Phys. **6**, 376 (2010).

[7] J. Maciejko, V. Chua, and G. A. Fiete, Phys. Rev. Lett. **112**, 016404 (2014).

[8] A. Rüegg and G. A. Fiete, Phys. Rev. Lett. **108**, 046401 (2012).

[9] Y. Tada, R. Peters, M. Oshikawa, A. Koga, N. Kawakami, and S. Fujimoto, Phys. Rev. B **85**, 165138 (2012).

[10] T. Yoshida, R. Peters, S. Fujimoto, and N. Kawakami, Phys. Rev. B **87**, 165109 (2013).

[11] J. C. Budich, B. Trauzettel, and G. Sangiovanni, Phys. Rev. B **87**, 235104 (2013).

[12] M. Hohenadler and F. F. Assaad, J. Phys.: Condens. Matter **25**, 143201 (2013).

[13] H.-H. Hung, V. Chua, L. Wang, and G. A. Fiete, Phys. Rev. B **89**, 235104 (2014).

[14] A. Shitade, H. Katsura, J. Kuneš, X.-L. Qi, S.-C. Zhang, and N. Nagaosa, Phys. Rev. Lett. **102**, 256403 (2009).

[15] S. Chadov, X. Qi, J. Kübler, G. H. Fecher, C. Felser, and S. C. Zhang, Nat. Mater. **9**, 541 (2010).

[16] H. Lin, L. A. Wray, Y. Xia, S. Xu, S. Jia, R. J. Cava, A. Bansil, and M. Z. Hasan, Nat. Mater. **9**, 546 (2010).

[17] B. Yan, L. Müchler, X.-L. Qi, S.-C. Zhang, and C. Felser, Phys. Rev. B **85**, 165125 (2012).

[18] J. C. Budich, R. Thomale, G. Li, M. Laubach, and S.-C. Zhang, Phys. Rev. B **86**, 201407 (2012).

[19] S. Rachel and K. Le Hur, Phys. Rev. B **82**, 075106 (2010).

[20] T. Yoshida, S. Fujimoto, and N. Kawakami, Phys. Rev. B **85**, 125113 (2012).

[21] T. Yoshida, R. Peters, S. Fujimoto, and N. Kawakami, Phys. Rev. Lett. **112**, 196404 (2014).

[22] S.-Q. Ning, H.-C. Jiang, and Z.-X. Liu, Phys. Rev. B **91**, 241105 (2015).

[23] M. Dzero, K. Sun, V. Galitski, and P. Coleman, Phys. Rev. Lett. **104**, 106408 (2010).

[24] V. Alexandrov and P. Coleman, Phys. Rev. B **90**, 115147 (2014).

[25] P. Nikolić, Phys. Rev. B **90**, 235107 (2014).

[26] B. Roy, J. D. Sau, M. Dzero, and V. Galitski, Phys. Rev. B **90**, 155314 (2014).

[27] V. Alexandrov, P. Coleman, and O. Erten, Phys. Rev. Lett. **114**, 177202 (2015).

[28] A. M. Lobos, A. O. Dobry, and V. Galitski, Phys. Rev. X **5**, 021017 (2015).

[29] M. Dzero, J. Xia, V. Galitski, and P. Coleman, Annu. Rev. Condens. Matter Phys. **7**, 249 (2016).

[30] A. Menth, E. Buehler, and T. H. Geballe, Phys. Rev. Lett. **22**, 295 (1969).

[31] S. Wolgast, C. Kurdak, K. Sun, J. W. Allen, D.-J. Kim, and Z. Fisk, Phys. Rev. B **88**, 180405 (2013).

[32] X. Zhang, N. P. Butch, P. Syers, S. Ziemak, R. L. Greene, and J. Paglione, Phys. Rev. X **3**, 011011 (2013).

[33] D. J. Kim, S. Thomas, T. Grant, J. Botimer, Z. Fisk, and J. Xia, Sci. Rep. **3**, 3150 (2013).

[34] P. P. Baruselli and M. Vojta, Phys. Rev. Lett. **115**, 156404 (2015).

[35] M. Legner, A. Rüegg, and M. Sigrist, Phys. Rev. Lett. **115**, 156405 (2015).

[36] J. Iaconis and L. Balents, Phys. Rev. B **91**, 245127 (2015).

[37] A. Mezio, A. M. Lobos, A. O. Dobry, and C. J. Gazza, Phys. Rev. B **92**, 205128 (2015).

[38] F. Haldane, Phys. Lett. A **93**, 464 (1983).

[39] F. D. M. Haldane, Phys. Rev. Lett. **50**, 1153 (1983).

[40] H. Tsunetsugu, Y. Hatsugai, K. Ueda, and M. Sigrist, Phys. Rev. B **46**, 3175 (1992).

[41] I. Hagymási, J. Sólyom, and Ö. Legeza, Phys. Rev. B **92**, 035108 (2015).

[42] T. Schork, S. Blawid, and J.-i. Igarashi, Phys. Rev. B **59**, 9888 (1999).

[43] P. Thalmeier, M. Siahatgar, B. Schmidt, and G. Zwicknagl, J. Korean Phys. Soc. **62**, 1388 (2013).

[44] N. Shibata, C. Ishii, and K. Ueda, Phys. Rev. B **51**, 3626 (1995).

[45] N. Shibata, C. Ishii, and K. Ueda, Phys. B (Amsterdam, Neth.) **223-224**, 363 (1996).

[46] E. Novais, E. Miranda, A. H. Castro Neto, and G. G. Cabrera, Phys. Rev. B **66**, 174409 (2002).

[47] S. R. White, Phys. Rev. Lett. **69**, 2863 (1992).

[48] S. R. White, Phys. Rev. B **48**, 10345 (1993).

[49] U. Schollwöck, Rev. Mod. Phys. **77**, 259 (2005).

[50] R. M. Noack and S. R. Manmana, AIP Conf. Proc. **789**, 93 (2005).

[51] K. Hallberg, Adv. Phys. **55**, 477 (2006).

[52] Ö. Legeza and J. Sólyom, Phys. Rev. B **68**, 195116 (2003).

[53] G. Vidal, J. I. Latorre, E. Rico, and A. Kitaev, Phys. Rev. Lett. **90**, 227902 (2003).

[54] P. Calabrese and J. Cardy, J. Stat. Mech. (2004) P06002.

[55] Ö. Legeza and J. Sólyom, Phys. Rev. Lett. **96**, 116401 (2006).

[56] J. Rissler, R. M. Noack, and S. R. White, Chem. Phys. **323**, 519 (2006).

[57] L. Amico, R. Fazio, A. Osterloh, and V. Vedral, Rev. Mod. Phys. **80**, 517 (2008).

[58] H. Li and F. D. M. Haldane, Phys. Rev. Lett. **101**, 010504 (2008).

[59] S.-J. Gu, S.-S. Deng, Y.-Q. Li, and H.-Q. Lin, Phys. Rev. Lett. **93**, 086402 (2004).

[60] L.-A. Wu, M. S. Sarandy, and D. A. Lidar, Phys. Rev. Lett. **93**, 250404 (2004).

[61] M.-F. Yang, Phys. Rev. A **71**, 030302 (2005).

[62] S.-S. Deng, S.-J. Gu, and H.-Q. Lin, Phys. Rev. B **74**, 045103 (2006).

[63] F. Pollmann, A. M. Turner, E. Berg, and M. Oshikawa, Phys. Rev. B **81**, 064439 (2010).

[64] A. M. Turner, F. Pollmann, and E. Berg, Phys. Rev. B **83**, 075102 (2011).

[65] F. Pollmann and A. M. Turner, Phys. Rev. B **86**, 125441 (2012).

[66] N. Shibata and K. Ueda, J. Phys.: Condens. Matter **11**, R1 (1999).

[67] Ö. Legeza, J. Röder, and B. A. Hess, Phys. Rev. B **67**, 125114 (2003).

[68] Ö. Legeza and J. Sólyom, Phys. Rev. B **70**, 205118 (2004).

[69] E. H. Kim, Ö. Legeza, and J. Sólyom, Phys. Rev. B **77**, 205121 (2008).

[70] C. Degli, E. Boschi, E. Ercolessi, and G. Morandi, in *Symmetries in Science XI* (Kluwer, Dordrecht, 2004), pp. 145–173.

[71] H. Tasaki, Phys. Rev. Lett. **66**, 798 (1991).